Experimental investigation on a Fe-Ga close yoke vibrational harvester by matching magnetic and mechanical biases

(Article begins on next page)

Research articles

Experimental investigation on a Fe-Ga close yoke vibrational harvester by matching magnetic and mechanical biases

S. Palumbo[a,b,c], P. Rasilo[d], M. Zucca[a,*]

[a] *Istituto Nazionale di Ricerca Metrologica, INRIM, Metrology for Quality of Life Dept, Strada delle Cacce 91, Torino, Italy*
[b] *Politecnico di Torino, Dipartimento di Elettronica e Telecomunicazioni, Corso Duca degli Abruzzi 24, Torino, Italy*
[c] *Istituto Italiano di Tecnologia, IIT, Graphene Labs, Via Morego, 30, Genova, Italy*
[d] *Tampere University of Technology, Laboratory of Electrical Energy Engineering, Korkeakoulunkatu 3, Tampere, Finland*

ABSTRACT

The output power generated by a vibrational magnetostrictive energy harvester depends on several parameters, some of them linked to the mechanical source, as vibration amplitude and frequency, others related to design quantities, like mechanical preload, magnetic bias, coil turns and load impedance. Complex models have been developed in literature to reproduce the behavior of these devices. However, for output variables such as power and voltage, one moves in a space of many variables and it is not trivial to reconstruct an overall behavior of the device.

The aim of this paper is to provide a wide picture concerning the device behavior investigating experimentally the output power and voltage as a function of the mechanical and especially magnetic bias, varying the amplitude and frequency of the driving vibration. A galfenol rod ($Fe_{81}Ga_{19}$) sample inserted in a three-legged magnetizer is utilized to vary the magnetic bias and to provide the flux closure to the sample, while a dynamic test machine provides both the mechanical bias and the driving vibration at different frequencies up to 100 Hz. The paper analysis has highlighted that the output power and voltage depend on the magnetic bias according to an exponentially modified Gaussian distribution. Keeping constant the other parameters and varying the mechanical bias, a family of modified Gaussian distributions is obtained. Moreover, fixing the electric load, the amplitude and frequency of the vibration, the couple of values "magnetic bias – mechanical preload" corresponding to the maximum output power of the device depicts a linear behavior.

The results here obtained point out that it is possible to simplify the design of magnetostrictive energy harvesters and to obtain high output power even with permanent magnets providing a relatively small coercive field. The results have been confirmed by using two yokes equipped with permanent magnets on the external columns. The maximum output average power obtained with permanent magnets has been 796 mW equal to 6.5 mW/cm^3 with a sinusoidal vibration amplitude of 40 MPa at 100 Hz.

1. Introduction

Energy harvesters (EHs) represent an ideal energy supply for wireless sensors, and especially for microelectromechanical systems, since they are able to generate electric energy using sources generally untapped (i.e. the exhaust heat or the vibrations generated by an engine) [1]. Electrostatic, electrodynamic and piezoelectric harvesters are the most common vibrational energy harvesters in these applications. Wang and Yuan perform a comparison in [2], where pros and cons of each device are discussed. Otherwise, giant magnetostrictive materials, such as amorphous metallic glass Metglas ($Fe_{81}B_{13.5}Si_{3.5}C_2$) [2], crystalline alloy Terfenol-D ($Tb_{0.3}Dy_{0.7}Fe_{1.9-2}$) [3,4] or galfenol ($Fe_{1-x}Ga_x$;

$x \sim 0.20$) [5], can provide a robust alternative with high power density [6]. Reference [7] illustrates an overview on recent achievements in the field of magnetostrictive energy harvesting. In particular, a comparison between galfenol and Terfenol-D [5] shows the better performances of the first one in vibrational energy harvesting applications where the mechanical excitation vibrational frequency is lower than 100 Hz. In addition, Fe-Ga provides a good compromise between magnetoelastic properties and workability. Galfenol's magnetostrictive properties have been widely analysed in literature, studying dependency on temperature [8], on stress annealing [9] and on crystalline texture [10,11]. Coupling coefficients have been discussed in [12]. In [13] and [14,15], the magnetic induction variation in a galfenol rod is studied versus the

---

applied stress as a function of different applied magnetic biases, neglecting the preload effect and applying the stress in quasi static conditions (1) Hz). The Fe-Ga vibrational EHs are proposed both as cantilever structure and as direct force arrangement. In cantilever harvesters, the magnetic bias is provided by a permanent magnet (PM), but few papers discuss the role of this parameter and none do it extensively. In [16] and [17] the performance of a cantilever transducer is analyzed by varying the resistive load. In [18], the output voltage of a PM unimorph energy harvester is experimentally analyzed as a function of a variable magnetic bias given using 0, 1, 2 and 3 PMs. In [19] the PM of a cantilever transducer is chosen by analyzing the magnetic bias effect through a finite element approach, based on experimental field-magnetization characteristics drawn as a function of stress.

In the direct force harvesters, where the vibrating force directly presses a Fe-Ga rod, a single pair of PMs is normally series or parallel connected to the rod thus providing the magnetic bias. In [5], the performance (output voltage and power) of the device is analyzed by varying the bias in steps, by using a variable number of permanent magnets (0, 4, 8, 12 and 16 PM's). In [20], where a three Fe-Ga rods harvester is presented, the variation of the magnetic bias is again obtained by varying from 1 to 4 the number of permanent magnets embedded in the magnetic closure. In [21] a Fe-Ga harvester is coupled to a C closure yoke fitted by an excitation coil that varies the magnetic bias up to saturation. In [22] a stressed annealed galfenol harvester is studied through a three port equivalent circuit validated by experimental measurements. The last two studies present interesting results but only with few measurement points and a limited vibration frequency lower than 1 Hz.

The study presented in this paper analyzes in detail the performance of a direct force harvester based on a polycrystalline galfenol sample (cubic grains with ⟨1 0 0⟩ easy axes) by varying finely the magnetic and mechanical bias and electrical load. In this paper it was preferred to consider galfenol unannealed, so as to make the applied preload values clear and evident, although stress annealed galfenol is interesting for energy harvesting as it is possible to design a device that does not require an external preload.

As in the case of the efficiency analysis of a Terfenol-D harvester performed in [23], the authors make use of an experimental setup mainly developed in [24], obtaining complete and clear characteristics of the harvester behavior.

The study was performed in a laboratory setup, keeping the preload constant by means of a test machine. This provides clear and reproducible results. However, in real applications the dynamic chain (rod, plus springs, plus non perfectly rigid encasing, etc.) leads to fluctuations in mechanical quantities that should be taken into account during the design phase.

The study clearly highlights the correlation existing between mechanical prestress and magnetic bias in the generation of the electrical power. This was possible by a laminated yoke designed to saturate the galfenol rod in dynamic conditions even at high prestress (up to 120 MPa). Another important feature of the present study is the use of excitation coils to produce the magnetic bias. Of course, the adoption of this solution, which requires an additional energy source, is not feasible in the actual harvesters, but it proves to be an essential tool for a detailed analysis because it allows a continuous regulation of the bias, in comparison with the stepped values provided by the permanent magnets. The choice of replacing the magnets with excitation coils has requested a verification that the results are not modified by this substitution. For such a purpose, two additional devices have been made by adopting yokes having the same size and the same laminations as in the yoke fitted with coils. The total length of galfenol rod is kept constant so that the laminated yokes of the external column are shortened to house two or four magnets respectively. It has been found out that, with a suitable tuning of the preload, the additional devices provide the same power obtained with the excitation coils. The values of electric power, bias and preload obtained with the permanent magnets are consistent with the values obtained by the yoke with coils and help one to better understand the behavior of the harvester.

We find out that the output power versus the magnetic field bias is shaped as an exponentially modified Gaussian distribution. A family of similar Gaussian distributions, shifted with respect to the magnetic bias, is obtained by varying the mechanical bias and keeping constant the other parameters. Moreover, for a given electric load and vibration amplitude and frequency, a linear relationship is found between the magnetic bias and the mechanical preload corresponding to the maximum output power.

These new results achieved are extremely useful for an efficient design of these devices, and they demonstrate that it is possible to maximize the output power with a minimum bias.

2. Experimental setup

2.1. Device layout with coils

In this paper, we characterized an axial force energy harvester under sinusoidal force excitation vibration. The harvester has a galfenol rod inserted into a three-legged magnetizer. The dimensions of the magnetic circuit have been defined to house two excitation coils on the external columns (Fig. 1) through which the magnetic field bias (H_b) can be finely tuned up to the saturation of the magnetostrictive material. The magnetizer has been designed using the non-linear finite element code 3D Opera by Cobham, including the magnetic characteristic of the silicon iron laminations in the yoke and the ones of galfenol measured during a previous characterization under different prestress [24]. Through a power amplifier, changing the excitation current, the magnetic bias is tuned at different levels, while a dynamic test machine provides both the mechanical bias and the driving vibration up to 100 Hz.

The yoke and the external limbs are composed of four equal L-shaped elements constituted by a stack of 0.60 mm thick non-oriented Fe-Si. The central leg is the Fe-Ga sample connected to the yoke by two pure iron rings. The magnetostrictive element is made up of a cylinder of 6 mm radius at the two ends, while in the center the radius is reduced to 3 mm for a length of 48 mm. Two series connected 600 turns coils are wrapped around the external limbs. A DC current up to 6 A, flowing in these coils, can produce saturation in the Fe-Ga alloy even under a compressive stress of about 120 MPa. Around the magnetostrictive rod a 2000-turns pick-up coil is wrapped giving to the sample the appearance of a uniform cylinder.

In addition to the yoke with coils, two other yokes were built, made with the same Fe-Si non oriented laminations 0.6 mm thick. The column length was shortened so as to accommodate 1 or 2 magnets on each column, leaving the total height and length of the yoke unchanged. In the following, the yoke with one magnet per column is named #A, while the one with two PMs per column is named #B (Fig. 2).

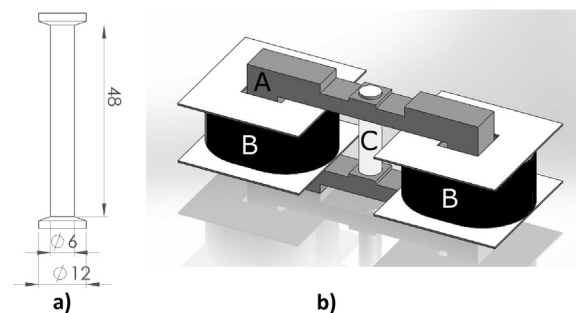We adopted a fatigue-testing machine (Instron, model E10000,

Fig. 1. a) Fe-Ga rod section. b) Three legged magnetizer harvester: A) Fe-Si 0.6 mm lamination magnetic closure, B) excitation coils, C) magnetostrictive Fe-Ga rod. The overall dimensions of the yoke are 120 mm × 68 mm × 15 mm.
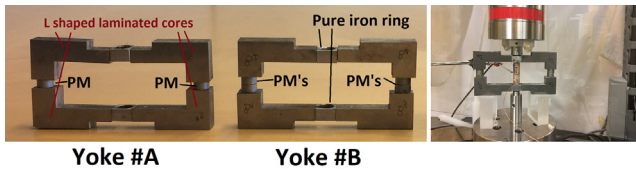
Fig. 2. Magnetic yokes with 2 (Yoke #A) and 4 (Yoke #B) permanent magnets. On the right side, yoke #B in the testing machine.
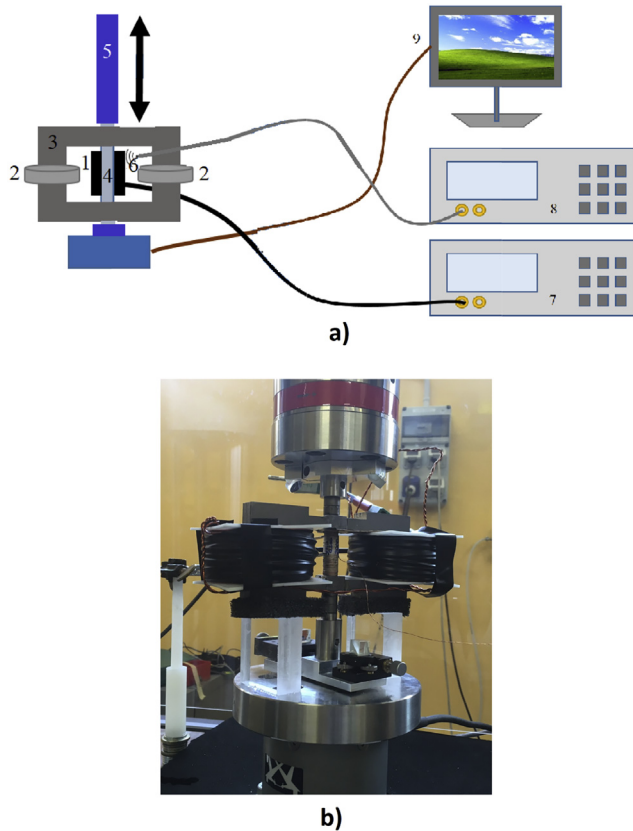

Fig. 3. a) Scheme of the measurement system. 1) Harvester pick-up coils, 2) Excitation coils, 3) Closure yoke, 4) Galfenol rod, 5) Test machine moving spindle, 6) Hall sensor, 7) Measuring system including programmable load resistors, 8) Mainframe Hall meter, 9) Control of the test machine including mechanical bias control and vibration amplitude. b) Picture of the device inserted in the test machine.

Instron Corp., Norwood, MA, USA) as a versatile solution to produce and control a sinusoidal mechanical vibration and, at the same time, to provide a constant mechanical bias. The scheme of the whole system and a picture of the device in the testing machine are reported in Fig. 3.

A control software (Instron Console and WaveMatrix software, Instron Corp., Norwood, MA, USA) sets the test parameters, such as mechanical preload (σ_0) and vibration amplitude ($\Delta\sigma_{pk}$). An additional software controls a signal generator (Agilent 33220A, Keysight Technologies, Santa Rosa, CA, USA) that, by means of a Kepco amplifier (BOP 72-6ML, Kepko Inc. Flushing, NY, USA), powers the coils to generate the desired bias. The magnetic field bias is measured by a Hall probe (Lakeshore 460, Lake Shore Cryotronics, Inc, Westerville, OH, USA) located next to the magnetostrictive material. The output power is dissipated on a programmable resistor (Pickering PXI 40-297- 002 programmable precision Resistors, Pickering Interfaces Ltd., Clacton-on-Sea, Essex, UK) and is measured, together with other electrical parameters, by a wattmeter Yokogawa WT 3000 (Yokogawa Electric Co., Musashino, Tokyo, Japan).
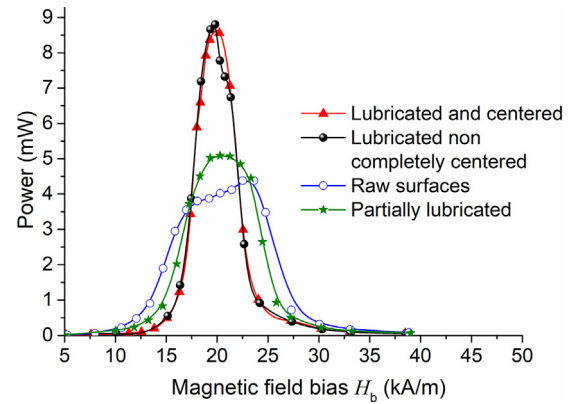

Fig. 4. Output power versus the applied magnetic field bias. Preload at 90 MPa. Vibration amplitude 4 MPa. Frequency of the vibration 100 Hz. Effect of friction and misalignment on the measurement results.

2.2. Device operation

The reproducibility of a measurement is the key point to obtain accurate results. In a fatigue-testing machine, the most important effect, which could affect the result accuracy, is the position of the sample with respect to the centre of the force. The machine, indeed, is projected to apply a uniaxial force on the sample, but when the latter is not centred, it could be subjected to a lower longitudinal force with spurious components. The friction between the harvester and the yoke is another cause of possible inaccuracies. In order to reduce this effect the gap should be increased to avoid an excessive friction, which is further amplified by the magnetic force between the sample and the yoke. However, on the other hand, the air gap should be minimized to increase the magnetization of the magnetostrictive sample. Thus, the only solution is to lubricate the contact surface between the magnetostrictive sample and the iron rings with a layer of lubricating grease.

Both the friction and the misalignment cause a significant variation on shape of the measurement results, as shown in the experimental curves of Fig. 4, where the diagrams in presence of these stray phenomena show a non-symmetric behaviour and a significant reduction of the maximum output power.

However, removing or reducing these effects, a symmetric curve is finally obtained. Lastly, to have the output power characteristics even at low preload values, in the detailed analysis of the next section we have limited the dynamic load amplitude below 10 MPa.

3. Experimental results with coils

The investigation aims, as specified in the introduction, to highlight the effect of the magnetic bias on the harvester performances. To do this, a first step was achieved by fixing the mechanical preload and by analyzing the output power versus the magnetic bias. By modifying the magnetizer excitation current, the bias is increased from about 5 kA/m to 40 kA/m and then reduced from 40 kA/m to 5 kA/m. The related curves of output power versus magnetic bias, presented in Fig. 5, are almost superimposed with differences between the two peaks values lower than 1%, proving that hysteresis phenomena are negligible. The output voltage, reported in the inset of Fig. 5, has a similar behavior.

The next experiments are performed keeping constant the vibration frequency (100 Hz) and the resistive load at 160 Ω The amplitude of the mechanical sinusoidal vibration is assumed to be constant, considering two values: 4 MPa and 8 MPa. The magnetic field bias ranges from zero up to 45 kA/m and the mechanical prestress is varied from 20 MPa to 120 MPa, using a 10 MPa step, for a total of 11 values. The results, summarized in Fig. 6, show a curve family of power versus magnetic bias, which well puts in evidence the strong correlation between magnetic and mechanical bias for an optimized behavior of the device.
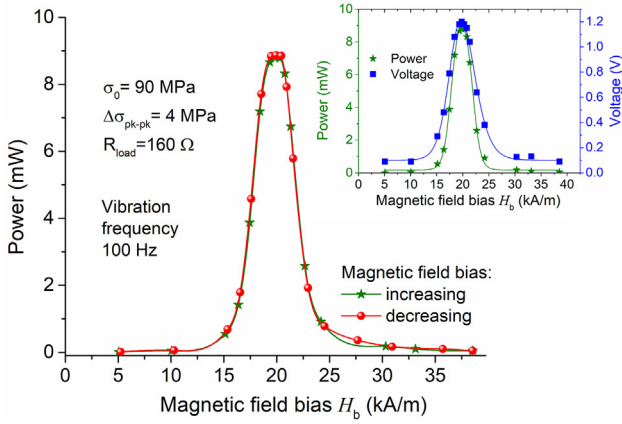
Fig. 5. Output power versus magnetic field bias, increasing and decreasing the latter and keeping constant the amplitude of the vibration excitation and of the mechanical preload. The inset shows, in comparison, the output voltage and power.
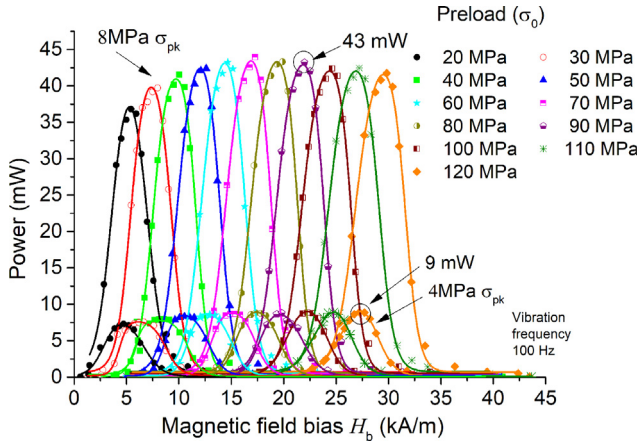

Fig. 6. Output power versus the magnetic field bias for different values of the mechanical preload and two values of the vibration amplitude. Dots represent the measurement points. Solid lines are the fits according to Eq. (1).

As expected, the output power depends on the vibration amplitude following a polynomial cubic law [4] while every curve can be described by an axisymmetric peak function, belonging to Gaussian family, as

$$P(H_b) = y_0 + \alpha P_{Max} \cdot \left(1 + e^{-\frac{H_b - H_c + w_1/2}{w_2}}\right)^{-1} \cdot \left[1 - \left(1 + e^{-\frac{H_b - H_c - w_1/2}{w_3}}\right)^{-1}\right]$$

(1)

where y_0 is an offset parameter having a value $< < 1$ mW. The parameter α depends on the mechanical preload with a value, in our experience, between $0.7 \leq \alpha \leq 1.0$. P_{Max} is the maximum output power in mW, i.e. the peak of the curve, while H_c is the value of the bias field expressed in kA/m corresponding to P_{Max}.

Finally, w_1, w_2 and w_3 are weights of the interpolator expressed in kA/m. As far as the interpolating coefficients are concerned, see Table 1 in the Appendix A. The behavior of the load voltage (V), which is related to the power according to $V(H_b) = \sqrt{P(H_b) \cdot R_{load}}$, is shown in the Appendix, Fig. A1.

The results shown in Fig. 6 also reproduce for greater amplitudes of mechanical vibration, as shown in Appendix C.

The above result shows how a high output power, when increasing the mechanical preload, implies an increase of the magnetic bias and vice versa. This is particularly evident plotting the peak values of the curve family of Fig. 6 in the plane H_b – σ_0. As Fig. 7 shows, there is a
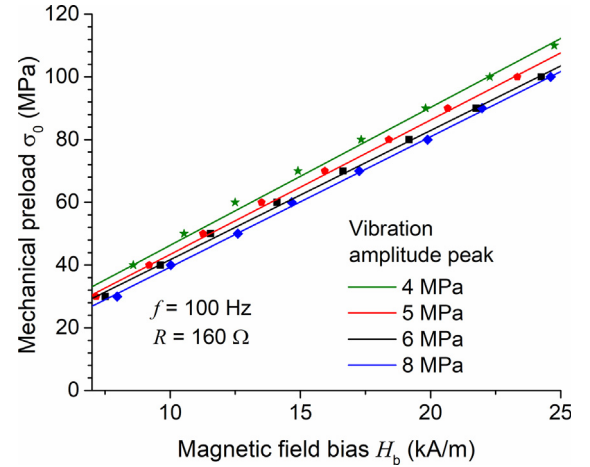

Fig. 7. Mechanical preload versus magnetic field bias of the maximum output power values (see Fig. 6 for vibration amplitudes peaks of 4 MPa and 8 MPa). Curve family obtained varying the vibration stress amplitude. Frequency of the vibration 100 Hz.

linear relationship between the two quantities. The results also prove that, for a given magnetic bias, the optimized device performances can always be obtained by simply adjusting the mechanical preload. In addition, in the design phase, since the relationship is linear it is sufficient to analyze only two points. This result, if confirmed also for the usual variations in the chemical composition of the galfenol produced in different batches, could simplify the design of these devices by means of prototypes or numerical codes, limiting the number of tests or simulations necessary for the project.

The trend of the output power shown in Fig. 6 can be explained by the behavior of the magneto-mechanical coupling factor (k) as a function of the same quantities. The coupling factor, introduced in [25], is a measure of the transduction efficiency of the Galfenol material and it is defined as the geometric mean of the actuator and sensor efficiencies (η_a, η_s). This quantity can be expressed in terms of the material properties as

$$k(\sigma, H) = \sqrt{\eta a \eta s} = \sqrt{\frac{d \cdot d^* \cdot E}{\mu}}$$

(2)

where d and d^* are the piezomagnetic coefficients, E is the Young modulus and μ is the magnetic permeability.

The coupling factor is related only to the transduction efficiency inside galfenol, without including the parasitic phenomena (dynamic losses, joule losses in the coil resistance, friction losses), which reduce the total efficiency of the whole harvester device. However, assuming in a first approximation the coupling factor as an efficiency parameter, its trend will be proportional to the output power for constant values of the mechanical input power and the influence parameters (temperature, frequency, electric load, coil turns and so forth). This consideration well justifies why the bell curves obtained by simulation in [25] are very similar to the experimental result shown in Fig. 6.

Fig. 8 shows the peak values of the output power as a function of the magnetic bias, for five different values of the vibration amplitude (4 MPa, 6 MPa, 8 MPa, 12 MPa and 16 MPa). The experimental points are efficiently interpolated using a parabolic curve. Fig. 8 highlights that, for a given vibration amplitude, there exists an absolute maximum of the output power given by a specific pair of values of magnetic and mechanical bias.

The curve family shown in Fig. 6 has been determined for a constant load resistance, which has been chosen as a matching load with a 23.8 kA/m bias and a 90 MPa preload. However, the matching electric load also varies depending on the magnetic bias. To analyze this variation, we kept constant the amplitude (8 MPa) and frequency (100 Hz)
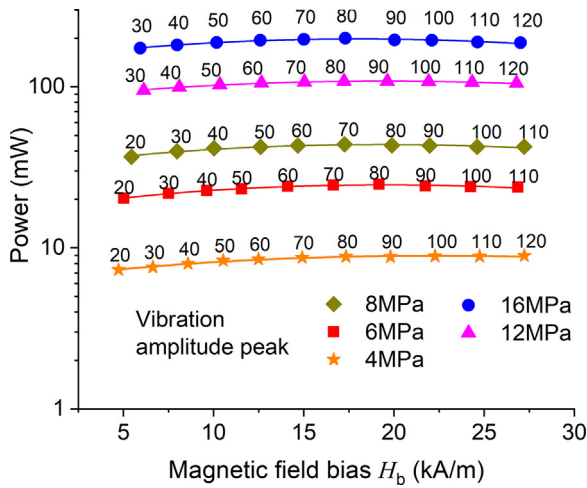
Fig. 8. Maximum output power versus the magnetic field bias for different preload values (labels near symbols). Curve family obtained by varying the vibration stress amplitude. Frequency of the vibration 100 Hz.
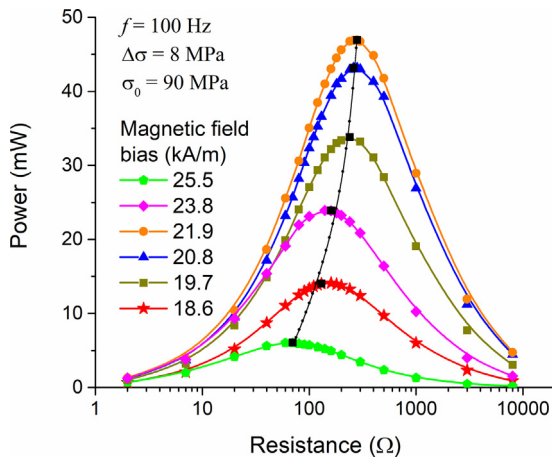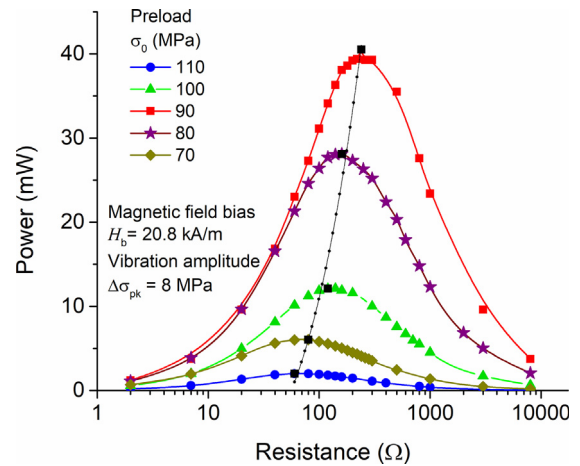

Fig. 10. Output power versus the load resistance values. Curve family obtained varying the mechanical preload and keeping constant the magnetic bias at 20.8 kA/m. Frequency of the vibration 100 Hz.
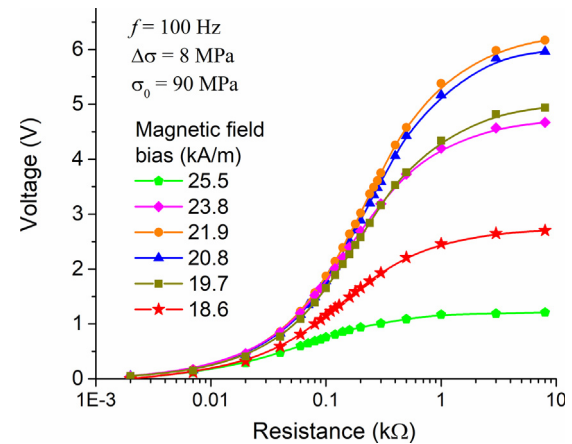

Fig.9. Output power versus the load resistance values. Curve family obtained varying the magnetic field bias and keeping constant the mechanical preload at 90 MPa. Frequency of the vibration 100 Hz.

Fig. 11. Output voltage versus load resistance. Curve family obtained varying the magnetic bias and keeping constant the mechanical preload at 90 MPa.

reported in Appendix E.

4. Experimental harvester results

of the vibration, the mechanical preload (90 MPa) and the magnetic bias (from 18.6 kA/m to 25.5 kA/m) and we measured the power output as a function of the load resistance R_{load}. Thus, considering some magnetic bias values, we obtained the family of bell-shaped curves versus R (in logarithmic scale) presented in Fig. 9.

While Fig. 6 gives important information for the design of the device, Fig. 9 shows that, as expected, a further optimization of the designed device can be made a posteriori by adapting, when possible, the electrical resistance as a function of bias and preload. For the considered harvester, for magnetic biases between 20 and 24 kA/m, the 2000 turn coil with winding resistance of 30.4 Ω shows an optimum resistive load between 160 and 280 Ω. In the same conditions, a 1000 turn coil shows an optimum resistive load between 20 and 65 Ω (see Appendix D).

For sake of completeness in Fig. 10 we have mapped the same curves for a constant magnetic bias assuming the prestress as a parameter.

Fig. 11 illustrates the voltage levels generated at 100 Hz in the same conditions as for Fig. 9, i.e. with 8 MPa vibration amplitude and 90 MPa preload, as a function of the load resistance. The diagram includes six curves related to six different magnetic bias values. It can be noted that, with load resistance above 200 Ω, the device can provide voltages between 1 and 6 V, depending on the magnetic bias. Current values are

The yoke equipped with coils allowed the analysis of the general behavior of the harvester, free from the limited bias imposed by permanent magnets, which are the magnetization source of a real harvester. In this second part of the paper, we focus on the operation of the harvester with permanent magnets. The two configurations considered, yoke #A, and yoke #B, allow one to impose two different magnetizations (bias) to the galfenol. Furthermore, it should be underlined that the two yokes have the same dimensions and are made of the same material as the yoke with coils, so that one can compare the results.

The magnetization imposed to the galfenol rod is not actually constant but, as we see later, it undergoes a limited variation due to the applied preload that, in turn, modifies the galfenol permeability.

The yoke #A and #B, fitted with same galfenol rod sample used for the previous investigations, have been analyzed under the same test conditions applied in Sect. II: sinusoidal vibration with frequency 100 Hz and σ_{pk} equal to 4 MPa and 8 MPa. The results are shown in Fig. 12 in terms of electrical output power versus the applied preload. The bell shape curve, at the vibration amplitude of 8 MPa, sees a maximum of the generated power equal to 40.9 mW at the prestress of 45 MPa for the yoke #A and 44.4 mW at the prestress of 55 MPa for the yoke #B. Taking into account possible slight differences in the
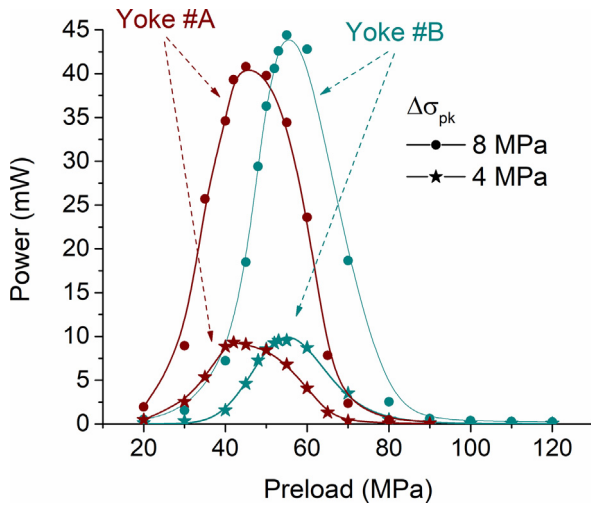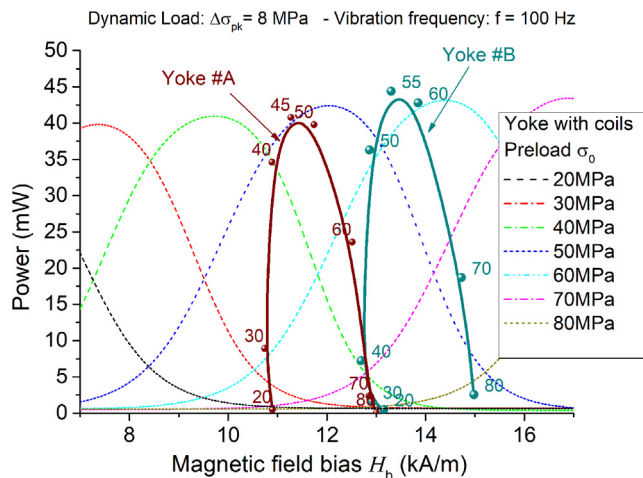
Fig. 12. Output power versus preload for the two harvesters with PM's. Curves obtained varying the preload for two different values of the vibration amplitude. Vibration frequency is 100 Hz. Load resistance 160 Ω.

construction of the yokes and within the limits of repeatability of the measurements, they are congruent with the maximum values of about 43.0 mW obtained with the coils. The same agreement is found for σ_{pk} equal to 4 MPa, where the maximum power is 9.30 mW and 9.55 mW for yoke #A and #B respectively, while that measured with the coils is about 9.0 mW with small variations as a function of preload.
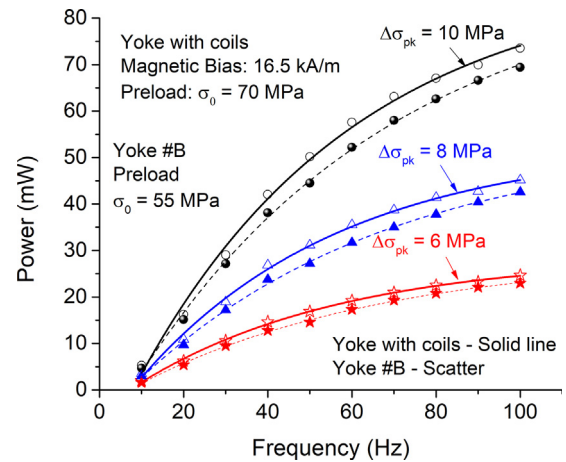
A second comparison with the configuration with the coils is shown in Fig. 13. This figure shows the generated power of the harvester as a function of the magnetic bias measured at the center of the galfenol rod. In the same figure, the trends of Fig. 6 relative to the yoke with coils are reported with dotted lines. A few remarks can be made:

- the bias applied to the galfenol sample by PM's varies with the preload from ~11 kA/m to ~13 kA/m for the configuration #A and between ~13 kA/m to ~15 kA/m for the configuration #B.
- the power values obtained at a given preload, are close to the corresponding curves at the same preload measured with the yoke with coils.

Experimental verification with magnets confirms that the bell

Fig. 13. Measured output power versus magnetic bias for the two harvesters with PM's. Curves obtained varying the preload (labels in MPa). Vibration amplitude $\sigma_{pk} = 8$ MPa. Frequency 100 Hz. Load resistance 160 Ω. The dotted curves are the ones measured with the yoke with coils and shown in Fig. 6. They are reported here for comparison.

curves shown in Fig. 6 are general feature of these devices. This result is particularly important because establishes that the optimized harvester does not require a magnet with specific and well defined characteristics, but the maximum output power can be reached by using any permanent magnet, provided that the preload is adapted to the corresponding magnetic bias.

The behavior versus frequency is defined by the curves of the output power and voltage presented in Figs. 14 and 15 respectively. These diagrams show the experimental results obtained both with coils and with magnets (yoke #B). In the case with coils, the magnetic bias is fixed at 16.5 kA/m and the preload to 70 MPa, which corresponds to the maximum power peak in the curve family of Fig. 6. In the case of yoke #B with four magnets, the conditions are the ones of the maximum power in Fig. 13 ($\sigma_0 = 55$ MPa). In both cases, the mechanical dynamic load is varied from 6 MPa to 10 MPa with 2 MPa step.

In all curves, both power and voltage decrease exponentially by decreasing frequency and their trend is interpolated by the exponential fit
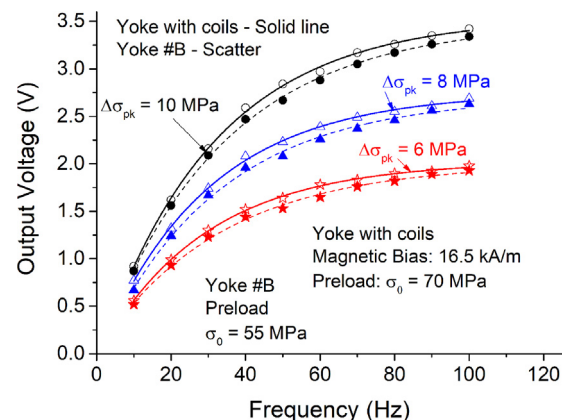
$$y(f) = Y_0 - A \cdot e^{-R_0 f} \qquad (3)$$

Fig. 14. Output power versus frequency. Curve families obtained varying the vibration amplitude $\Delta\sigma_{pk}$ to these values: 6 MPa, 8 MPa and 10 MPa. Three curves are related to the yoke with coils (solid lines with scatters), measured in the conditions of maximum output power at 70 MPa prestress. The other three curves are related to yoke #B with PM's, measured at the maximum power obtained with prestress equal to 55 MPa.

Fig.15. Output voltage versus frequency. Curve families obtained varying the vibration amplitude $\Delta\sigma_{pk}$ to these values: 6 MPa, 8 MPa and 10 MPa. Three curves are related to the yoke with coils (solid lines with scatters), measured in the conditions of maximum output power at 70 MPa prestress. The other three curves are related to yoke #B with PM's, measured at the maximum power obtained with prestress equal to 55 MPa.
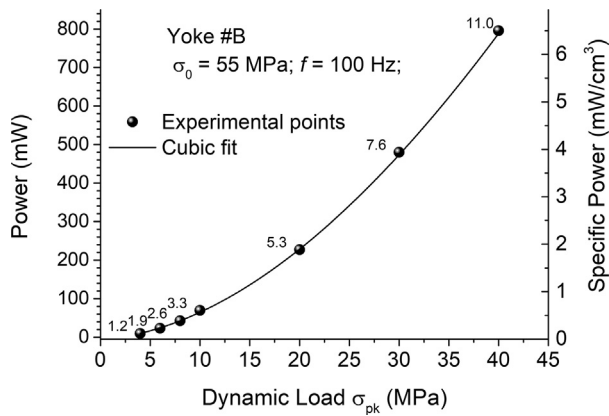
Fig. 16. Measured output power and specific power versus the applied dynamic load. Curve related to the yoke with permanent magnets (yoke #B). Frequency 100 Hz, mechanical prestress 55 MPa. The labels near the experimental points represent the measured output voltage in volt.

where Y_0 is the asymptotic value (in mW or V), A is a constant with the same dimension (in this case A close to Y_0) and R_0 is the rate. The diagrams of Figs. 14 and 15, where the experimental values (dots) are superimposed to the interpolated curve (continuous), both for yoke with coils and yoke #B, proves the excellent approximation of the fit.

The results of the harvester and of the yoke with coils agree satisfactorily. Since the harvester provides a voltage higher than 1 V beyond 20 Hz, it is able to supply an AC/DC converter when a conditioning circuit for a battery charge is required.

Fig. 16 shows the trend of the output power delivered by the device with PM's (Yoke #B), increasing the dynamic load σ_{pk} up to 40 MPa. The maximum specific power here obtained is equal to 6.5 mW/cm^3.

5. Discussion

This paper aims at deepening the analysis of the effects of magnetic field bias correlated with mechanical prestress on the performances of a direct-force galfenol harvester fitted with a close magnetic circuit, an aspect up to now less discussed in literature. An experimental setup, specifically suitable for such a purpose and carefully realized to ensure measurement repeatability, has allowed us to measure the evolution of the device output voltage and power for a fine variation of the magnetic bias up to saturation. At the same time, we have evaluated the role of several parameters of influence, as the mechanical prestress (up to 120 MPa), the vibration frequency (in a range between 10 Hz and 100 Hz), the vibration amplitude (from 4 MPa to 40 MPa) and the load

resistance (from 7 Ω to 10 kΩ).

The experiments performed varying the bias with coils prove that the relationship between output power (or voltage) and magnetic field bias is always described by a bell curve showing that a well-defined optimal condition can be always identified tuning the mechanical prestress as a function of the magnetic bias. The variation of the parameters of influence (mechanical preload, vibration frequency and amplitude, load resistance) changes of course the values of the output quantities, but does not modify the shape of the function output power (or voltage) versus magnetic bias. Such a result is particularly important because it highlights how an optimal output voltage/power can be always reached with low PM remanence, provided that the preload and the electrical load impedance are adequately tuned. Indeed, keeping constant the other parameters, low magnetic bias should be coupled with a low mechanical prestress, and vice versa, as clearly shown in Fig. 8.

The general behavior of the output power and voltage, of the harvester equipped with the joke with coils, can be justified looking at the behavior of the magneto-mechanical coupling factor.

The results have been confirmed by testing the same harvester with permanent magnets inserted in the yoke instead of coils. Similar output voltage trends as well as maximum out power values have been obtained.

Another interesting result, attained thanks to the large amount of data collected, is the locus of the points, represented in the plane $H_b – \sigma_0$, of the maximum output power values obtained for different vibration amplitudes. Such loci are represented by parallel straight lines and this result could significantly simplify the design of the device as two measuring points or simulations are sufficient to identify a characteristic.

Another result to highlight is that the device output voltage can be easily leaded to satisfy, even at low frequency, the minimum voltage required to couple the system to a rectifier. Finally, the device under investigation has provided a significant average output power equal to 796 mW, corresponding to a specific power of 6.5 mW/cm^3 under the following conditions: frequency 100 Hz, vibration amplitude 40 MPa, preload equal to 55 MPa.

Appendix

A. Fitting parameters

In Table 1 the fitting parameters concerning the family curves of Fig. 6 are presented, according to (1).

B. Voltage curve family

The voltage vs. the applied magnetic bias is presented in Fig. A1 for two different vibration amplitudes of 4 MPa and 8 MPa at constant preload. Eleven preload values are considered for a total of 22 curves. The diagram is the companion diagram of Fig. 6, concerning the output power.

C. Additional curve family

The diagrams of Fig. 6. can be also measured with greater amplitudes of the mechanical vibration, with a slight reduction in repeatability. Fig. A2. shows as an example the family of output power vs magnetic bias curves as a function of different preload values for a vibration amplitude of 20 MPa.

Table 1
Fig. 6 curves fitting parameters.

Δ σ(pk) MPa	σ0 MPa	y0 mW	Hc kA/m	Pmax mW	α	w1 kA/m	w2 kA/m	w3 kA/m
8	20	0.63	0.53	44.92	0.83	0.33	0.08	0.08
8	30	0.68	0.73	42.98	0.92	0.39	0.07	0.06
8	40	0.37	0.96	43.44	0.94	0.42	0.07	0.06
8	50	0.42	1.19	46.59	0.91	0.41	0.08	0.06
8	60	0.52	1.42	47.40	0.91	0.42	0.08	0.06
8	70	0.49	1.67	46.57	0.93	0.44	0.08	0.06
8	80	0.56	1.91	45.75	0.94	0.45	0.08	0.06
8	90	0.56	2.16	45.31	0.95	0.46	0.08	0.06
8	100	0.53	2.41	44.29	0.95	0.48	0.08	0.06
8	110	0.75	2.67	44.98	0.93	0.48	0.09	0.07
8	120	0.69	2.92	44.47	0.94	0.48	0.09	0.06
4	20	0.07	0.47	8.48	0.85	0.38	0.07	0.09
4	30	0.19	0.65	7.66	0.99	0.44	0.04	0.07
4	40	0.11	0.83	7.88	1.00	0.51	0.05	0.07
4	50	0.17	1.07	8.88	0.95	0.42	0.05	0.07
4	60	0.18	1.29	9.11	0.95	0.42	0.05	0.07
4	70	0.18	1.52	9.35	0.93	0.42	0.06	0.07
4	80	0.17	1.75	9.66	0.92	0.42	0.07	0.07
4	90	0.17	1.98	9.67	0.91	0.41	0.07	0.09
4	100	0.17	2.22	10.60	0.84	0.38	0.08	0.08
4	110	0.14	2.47	12.39	0.72	0.32	0.11	0.08
4	120	0.14	2.72	12.83	0.70	0.31	0.11	0.08
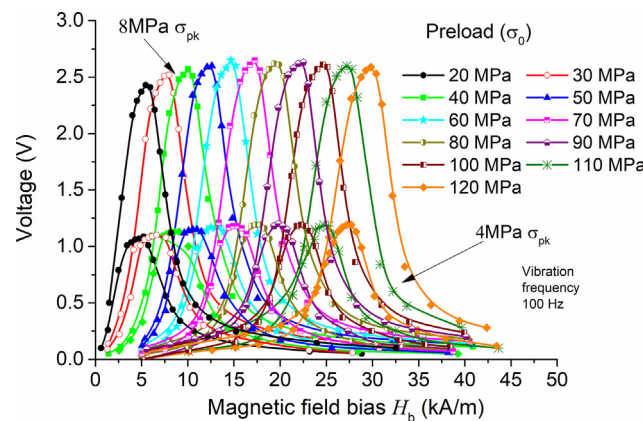
Fig. A1. Voltage versus the magnetic field bias for different values of the mechanical preload and two values of the vibration amplitude. Yoke with coils.
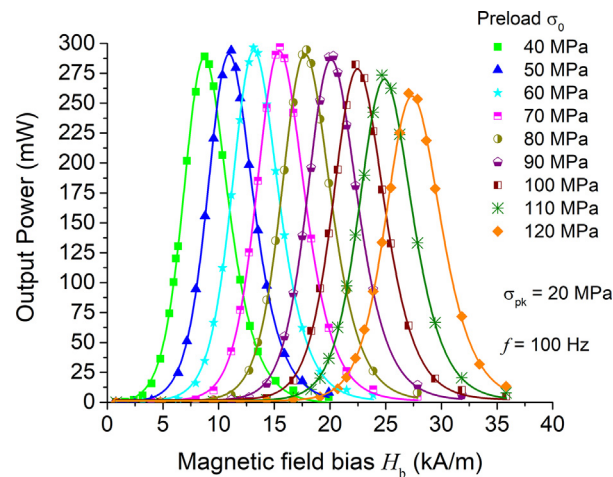
Fig. A2. Output power versus the magnetic field bias for different values of the mechanical preload at 20 MPa vibration amplitude. Yoke with coils. Dots represent the measurements points. Solid lines are the fits according to Eq. (1).
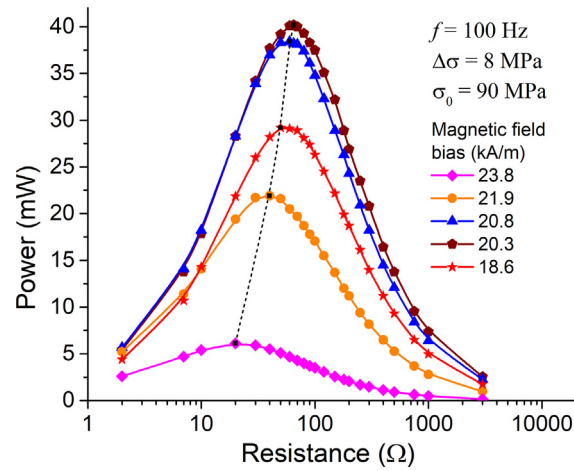
Fig. A3. Output power versus the load resistance values. Coil with 1000 turns. Curve family obtained varying the magnetic field bias and keeping constant the mechanical preload at 90 MPa. Frequency of the vibration 100 Hz.
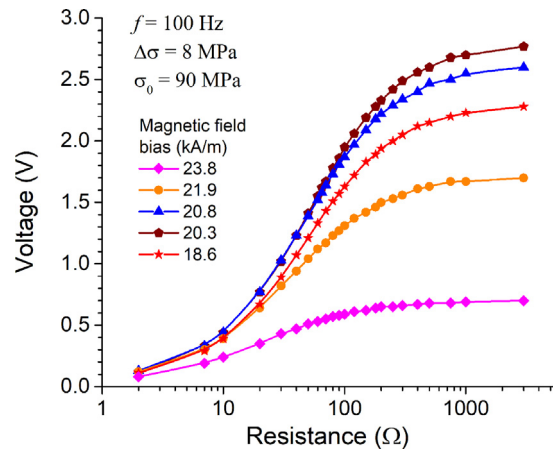

Fig. A4. Output voltage versus load resistance for the 1000 turns coil. Curve family obtained varying the magnetic bias and keeping constant the mechanical preload at 90 MPa.
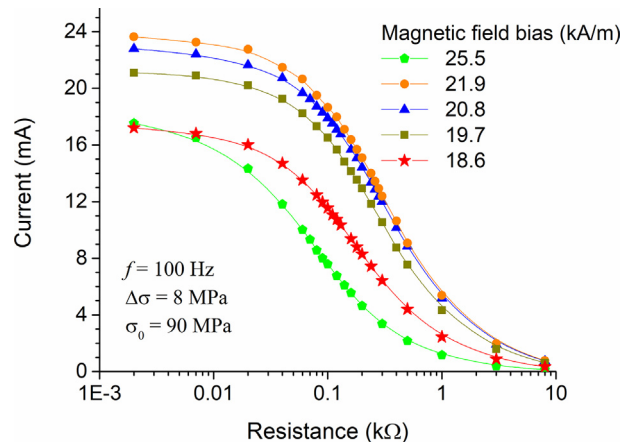

Fig. A5. Current versus load resistance for different values of the magnetic field bias at constant preload (90 MPa), vibration frequency (100 Hz) and vibration amplitude (8 MPa). Yoke with coils.

D. Output power versus load resistance

Fig. 9 shows the output power versus load resistance. Such a behaviour depends on the internal impedance of the harvester, which is also dependent on the mechanical and magnetic biases. As well known, when the load resistance matches the internal impedance the output power is maximum. The designer can choose the diameter of the wire and the number of turns depending on the desired output voltage and impedance. By way of example, here it is considered a coil having halved number of turns (1000), with a resistance of 10.4 Ω instead of 30.4 Ω and a wire diameter of 0.25 mm instead of 0.20 mm. The results in terms of matching load resistance and output voltage are reported in Figs. A3 and A4, respectively.

E. Current behaviour versus load resistance

While the load voltage increases when the load impedance rises (see Fig. 11), the current decreases according to an exponential trend. For different values of the magnetic bias field the curves in logarithmic scale are shown in the Fig. A5.

References

[1] S. Roundy, P.K. Wright, J. Rabaey, A study of low level vibrations as a power source for wireless sensor nodes, Comput. Commun. 26 (11) (2003) 1131–1144, https://doi.org/10.1016/S0140-3664(02)00248-7.

[2] Lei Wang, F.G. Yuan, Vibration energy harvesting by magnetostrictive material, Smart Mater. Struct. 17 (2008) 045009.

[3] M. Zucca, A. Hadadian, O. Bottauscio, Quantities affecting the behaviour of vibrational magnetostrictive transducers, IEEE Trans. Magn. 51 (2015) 8000104 (p. 1-4).

[4] M. Zucca, O. Bottauscio, Hysteretic modeling of electrical micro-power generators based on villari effect, IEEE Trans. Magn. 48 (2012) 3092–3095.

[5] V. Berbyuk, "Vibration energy harvesting using galfenol-based transducer, Act. Passive Smart Struct. Integr. Syst. SPIE 8688 (2013) 17–22.

[6] S. Beeby, N. White, Energy Harvesting for Autonomous Systems, Aterch House, Norwood (MA-USA), 2010, p. 91.

[7] Z. Deng, M. Dapino, Review of magnetostrictive vibration energy harvester, Smart Mater. Struct. 26 (2017) 1–18.

[8] R.A. Kellogg, A.B. Flatau, E. Clark, M. Wun-Fongle, T.A. Lograsso, Temperature and stress dependencies of the magnetic and magnetostrictive properties of $Fe_{0.81}Ga_{0.19}$, J. Appl. Phys. 19 (2002).

[9] M. Wun-Fogle, J.B. Restorff, A.E. Clark, E. Dreyer, E. Summers, Stress annealing of Fe-Ga transduction alloys for operation under tension and compression, J. Appl. Phys. 97 (2005).

[10] L. Weing, T. Walker, Z. Deng, M.J. Dapino, B. Wang, Major andminor stress-magnetization loops in textured polycrystalline $Fe_{81.6}Ga_{18.4}$ Galfenol, J. Appl. Phys. 113 (2013).

[11] A.E. Clark, J.B. Restorff, M. Wun-Fogle, T.A. Lograsso, D.L. Schlagel, Magnetostrictive Properties of Body-Centered Cubic Fe-Ga and Fe-Ga-Al alloys, IEEE Trans. Magnets 36 (2000).

[12] J.H. Yoo, G. Pellegrini, S. Datta, A.B. Flatau, An examination of Galfenol mechanical-magnetic coupling coefficients, Smart Mater. Struct. 20 (2011).

[13] P.G. Evans, M.J. Dapino, Measurement and modelling of magnetic hysteresis under field and stress application in iron–gallium alloys, J. Magn. Magn. Mater. 330 (2012) 37–48.

[14] J. Atulasimha, A.B. Flatau, Experimental actuation and sensing behavior of single-crystal iron-gallium alloys, J. Intell. Mater. Syst. Struct. 19 (2008) 1371.

[15] J. Atulasimha, A.B. Flatau, A review of magnetostrictive iron–gallium alloys, Smart Mater. Struct. 20 (2011).

[16] T. Ueno, S. Yamada, Performance of energy harvester using iron-gallium alloy in free vibration, IEEE Trans. Magn. 47 (2011).

[17] T. Ueno, Performance of improved magnetostrictive vibrational power generator, simple and high power output for practical applications, J. Appl. Phys. 117 (2015).

[18] Z. Deng, M.J. Dapino, Modeling and design of Galfenol unimorph energy harvesters, Smart Mater. Struct 24 (2015) 1–14.

[19] Z. Yang, Y. Tan, J. Zu, A multi-impact frequency up-converted magnetostrictive transducer for harvesting energy from finger tapping, Int. J. Mech. Sci. 126 (2017) 235–241.

[20] C.S. Clemente, D. Davino, C. Visone, "Experimental Characterization of a Three rods magnetostrictive device for Energy Harvesting, IEEE Trans. Magn. (2017).

[21] D. Davino, A. Giustiniani, C. Visone, A. Adly, Energy harvesting tests with galfenol at variable magneto-mechanical conditions, IEEE Trans. Magn. 48 (2012).

[22] C.S. Clemente, A. Mahgoub, D. Davino, C. Visone, Multiphysics circuit of a magnetostrictive energy harvesting device, J. Intell. Mater. Syst. Struct. 28 (2017) 2317–2330.

[23] M. Zucca, L. Callegaro, A setup for the performance characterization and traceable efficiency measurement of Magnetostrictive harvesters, IEEE Trans. Instrum. Meas. 64 (6) (2015) 1431–1437.

[24] M. Zucca, P. Mei, E. Ferrara, F. Fiorillo, Sensing dynamic forces by Fe-Ga in compression, IEEE Trans. Magn. 53 (11) (2017) 1–4.

[25] S. Datta, J. Atulasimha, A.B. Flatau, Figures of merit of magnetostrictive single crystal iron-gallium alloys for actuator and sensor applications, J. Magn. Magn. Mater. 321 (2009) 4017–4031.